Journal of Materials Chemistry A

Accepted Manuscript

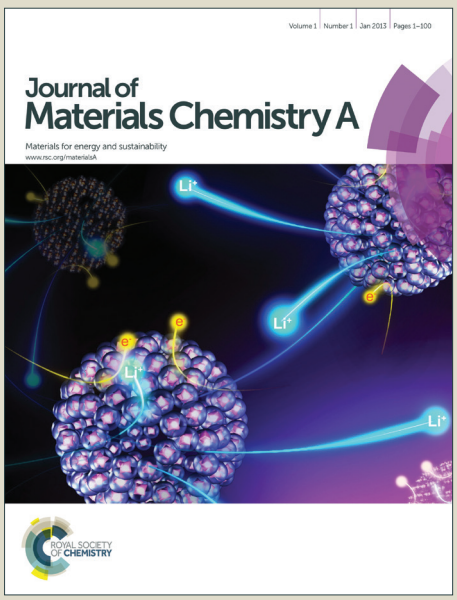

ROYAL SOCIETY OF CHEMISTRY

www.rsc.org/materialsA

Cite this: DOI: 10.1039/c0xx00000x

www.rsc.org/xxxxxx

ARTICLE TYPE

Graphene Based Composite Supercapacitor Electrodes with Diethylene glycol as Inter-layer Spacer

Yu Yu,[a] Yongbin Sun,[b] Changyan Cao,[a] Shuliang Yang,[a] Hua Liu,[a] Ping Li,[a] Peipei Huang,[b] and Weiguo Song*[a]

Received (in XXX, XXX) Xth XXXXXXXXX 20XX, Accepted Xth XXXXXXXXX 20XX
DOI: 10.1039/b000000x

Diethylene-glycol/Graphene nano-composites were produced by a simple mild solvothermal method, in which diethylene glycol was grafted onto the surfaces of reduced graphene oxides (RGO) as inter-layer spacer to spatially separate graphene sheets, i.e. to prevent the aggregation of graphene single sheets. The presence of diethylene glycol was confirmed by several characterizations including IR, XPS, and AFM. Because of the chain length and electrolyte affinity of diethylene glycol spacer, most of the surface area of graphene single layer sheets could be accessed by electrolyte, leading to high capacity as supercapacitors electrodes with a impressive electrochemical capacitance (237.8 F/g at a charging current of 0.1 A/g), outstanding rate performances (182.9 F/g at 20 A/g), and excellent cycling stabilities (less than 5 and 10% decline after 2000 and 10000 cycles). It is hence particularly promising for "high-power densities" and "long cycle life" supercapacitors electrodes.

Due to their long cycle life and rapid charging and discharging rate at high power densities, supercapacitors has continued to attract considerable attentions.[1] Graphene is a suitable candidate material for supercapacitors electrodes, especially for electrochemical double-layer capacitors because of its high electrical conductivity, mechanical strength, and large specific surface area.[2] Many approaches have been reported to produce graphene-based supercapacitors electrodes materials. Conducting polymers (e.g., polyaniline,[3] polypyrrole,[4] polythiophene) were widely employed to construct nanocomposites with graphene. These conducting polymers not only provide pseudo-capacitance but also improve the wetting between graphene and electrolytes due to their hydrophilic nature. Several advanced exfoliation methods[5] as well as other novel technologies (e.g. LBL assembly,[6] supercritical drying,[7] activation[8]) were also effective means. However, for such double layer capacitor, the effective surface area of the electrode materials was the key for high performance. For graphene sheets, they are prone to stick together through aggregation, resulting in poor wetting between reduced electrodes and electrolytes, and consequently reduced capacitance. Thus methods to spatially separate the graphene sheets were critical. We found that diethylene glycol was an outstanding spacer for this purpose.

Surface functional groups on the graphene could provide pseudo-capacitance and improve electrolyte affinity.[9] These functional groups could act as the "stabilizer" or "spacers" into the graphene layers to inhibit the agglomeration of reduced graphene sheets.[10] Ruoff produced a RGO electrode by dispersing GO in propylene carbonate followed by post-reduction.[11] Wong thermally treated the GO dispersed in dimethyl formamide at a moderate temperature to finely control of the density of functional groups.[12] Both of these RGO showed considerably improved performances as super capacitors. Others reagent (e.g., hydroquinone,[13] aqueous alkali solutions,[14] reducing sugar,[15] ionic liquid[9,16]) were also used as the reducer and solvent for similar purpose. However, the development of a facile, efficient and safe preparation of high-performance and low-cost supercapacitors electrode materials still makes a great deal of sense.

Here we report a facile solvothermal method to prepare a high performance RGO electrode. Diethylene glycol (DEG) was chosen to reduce and modify the GO surface. The absence of typical strong reducing agent and the relatively low temperature allows DEG to reduce GO to an appropriate extend, as well as being grafted onto graphene sheet. Suitable molecular length of DEG resulted in suitable spaces between graphene sheets to prevent aggregation, and the oxygen-containing groups on DEG lead to favourable wetting properties for electrolyte solution so that maximum portion of graphene sheets could be involved in charge storage. On such composite electrode material, a specific capacitance up to 237.8 F/g was achieved at 0.1 A/g. No obvious decline of capacity was observed when the current increased from 0.5 A/g to 20 A/g and cycles reached up to 2000 times.

Despite a certain viscosity, DEG is a relatively good solvent with affinity to the hydrophilic GO. By sufficient stirring and ultrasonication, GO could disperse in DEG thoroughly to form a uniform brown-colored suspension (Fig. S1a). The suspension of 0.3 mg/mL concentration turned into black after solvothermal treatment at 150 °C for 10 h in a Teflon-lined autoclave, indicating that assured reduction happened to GO. Meanwhile, as the Scheme 1, the DEG molecules were linked to graphene by chemical bonding, which will be elaborated thereinafter. We denoted hence the product as DEG/graphene. As both of scanning electron microscope (SEM) and scanning electron microscope (TEM) images showed (Fig. 1a, b), a sheet-like morphology similar to graphene was maintained in the black DEG/graphene, even after freeze drying. There were no particles or other

aggregation structures found in the field of vision. The dried DEG/graphene could be redispersed in water or ethanol by ultrasonication without precipitation for weeks (Fig. S1b, c). The homogeneous micrometer-sized DEG/graphene flakes were also measured by atomic force microscopy (AFM) to acquire the depth.

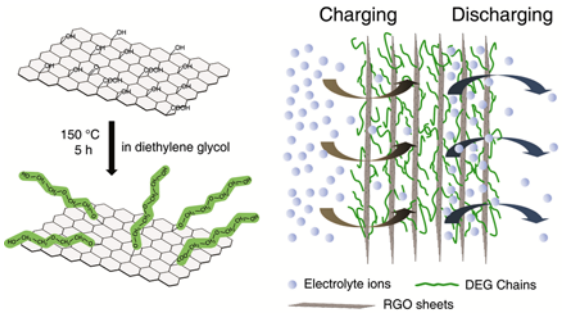

Scheme. 1 Schematic illustration of the conjunction of DEG and RGO dispersed in the diethylene glycol. The right scheme shows that the DEG molecule chains grafted into the RGO sheets introduce suitable porosity into multilayered graphene structure as the "spacers".

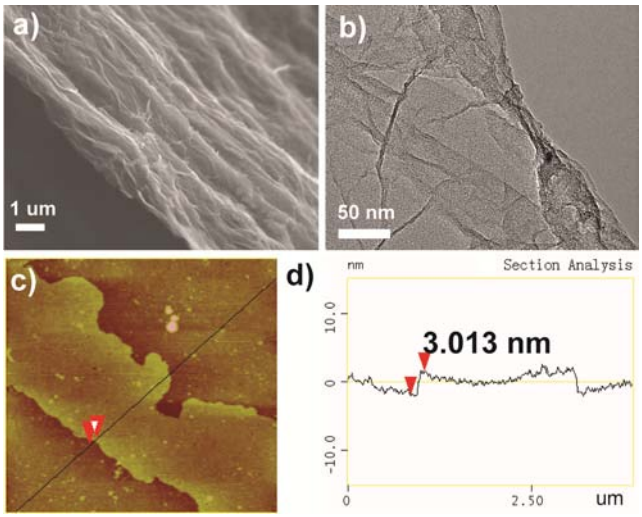

Fig. 1 Typical SEM (a) and TEM (b) images of DEG/graphene. (c) AFM ichnography and (d) cross-section contour of an individual DEG/graphene flake.

Fig. 1c presents a typical AFM image of an individual DEG/graphene flake, and it is clearly seen from the corresponding contour profile that the flake has a depth of about 3.013 nm (Fig. 1d). The original GO were also measured to make a comparison, most of which showed a depth of about 1.029 nm (Fig. S2). Such a depth demonstrated the pristine GO of nature of a single layer.[2a,17] The increasing of depth for DEG/graphene may not be attributed to stacking of single layers to two layers or three. For there were no stagger areas in the edge region of DEG/graphene, and their depths dispersed in a relatively concentrated area. Consequently, we deduced the DEG/graphene flakes should be homogeneously a single layer structure as their parent materials. The excess of DEG/graphene to GO in depth should be brought about by the graft of abundant functional groups with larger size.

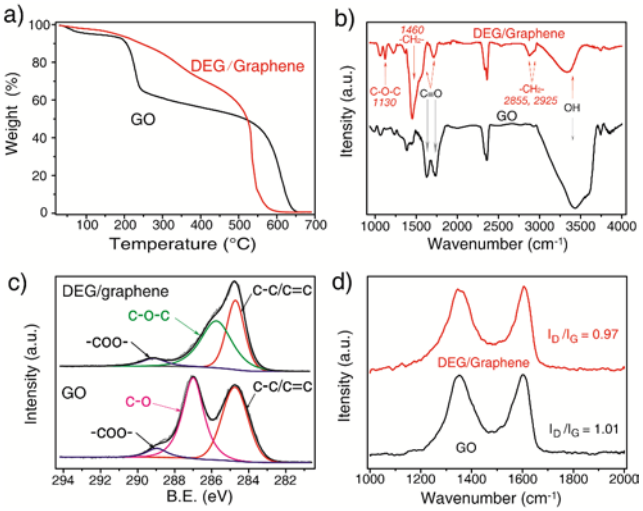

Fig. 2 TGA results (a), FTIR spectra (b), XPS of C1s (C), and Raman spectroscopy (d) of GO and DEG/graphene.

We investigated the interaction between RGO and DEG by a set of structural characterizations, including thermal gravimetric analysis (TGA), Fourier transform infrared spectroscopy (FTIR), X-ray photoelectron spectroscopy (XPS), and Raman spectroscopy. TG curve of pristine GO shown in Fig. 2a was very similar to that in other literatures,[18] as the little initial weight loss under 100 °C was due to the desorption of physical-adsorbed H_2O and EtOH volatile. There was a dramatics weight loss about 30% at 200 °C, arising from the decomposition of liabler oxygen-containing groups in GO (e.g. hydroxyl and carboxyl). Another dramatics weight loss at about 600 °C was indexed to completely decompose of conjugate areas. In contrast, DEG/graphene followed a slow and continuous weight loss from 100 °C to 500 °C originating from the multistep decomposition of DEG molecules grafted with RGO.[19] The slower weight loss suggested ether groups have relatively high thermal stability in air atmosphere, however, the thorough decompose of graphene was brought forward to 530 °C. The TG results of DEG and physically mixed DEG&RGO (Fig S3a) both showed DEG molecules volatilized before 200 °C. The conjunction between DEG and graphene was confirmed by IR spectra. As shown in Fig. 2b, GO showed an intensive and broad band at 3000-3700 cm^{-1} and distinct bands at 1730 and 1620 cm^{-1}, corresponding to hydroxyls and carbonyls (carboxylic) respectively.[20] After the solvothermal treatment, all of the three bands decreased sharply, and new partially overlapping bands at 2855 and 2925 cm^{-1} ascribing to the symmetric and asymmetric CH_2-stretching bands of methylene units appeared. Also a new strong band at 1461 cm^{-1} was dominated by the CH_2-scissoring modes of the ether methylene units, and the C-O-C stretching vibration gives an emerging absorption band at 1130 cm^{-1}.[21]

Both the C1s XPS spectra of GO and DEG/Graphene by peak fitting indicate the presence of three types of carbon bonds (Fig. 2c). The peak at 284.6 eV represented for C/C=C in the unoxidized aromatic region, and that at 289.0 eV stood for O-C=O of carboxyl.[9,22] The difference between the GO and DGE/graphene was that a characteristic peak of C-O at 287.0 eV deriving from the surface hydroxyls on the benzene ring was substituted by a characteristic peak at 286.0 eV corresponding to

the ether carbon atoms C-O-C.[23] In Raman spectra (Fig. 2d), the intensities ratio of two prominent bands around 1340 and 1580 cm^{-1} assigned to the D and G bands in GO and DEG/graphene displayed no obvious change (1.01 and 0.97 respectively), indicating that the size of graphitic domains with ordered conjugated structures didn't increase in EGD/graphene.[12] Accompanied with the information from XPS, we could conclude the oxygen-containing groups didn't be removed completely by the solvothermal treatment with DEG, but bonded with the DEG molecule by dehydration with the hydroxyls and carboxyls of DEG. As hydrophilic molecules, the grafted DEG molecules could guarantee the wetting between graphene and electrolytes. The static water contact angle of DEG/graphene film was 55.7° in the infiltration test (Fig. S4), which demonstrated wetting of GO could be achieved DEG, as other organic solvents. [24]

The agglomeration often happened to these RGO with substantial loss in oxygen-containing groups during the chemical reduction, which will decrease the surface area and access of electrolyte ions to the surface of the RGM sheets.[25] Due to the presence of a great quantity of larger and more stable groups on the graphene sheet, the DGE/graphene could avoid the serious agglomeration due to the decline of electrostatic repulsions between RGO sheets, and play a great role as the "spacers", introducing suitable porosity into multilayer. As shown in Fig. S5, our DEG/graphene after freeze drying provided a type-IV isotherm with a specific surface area as 665.5 m^2/g and pore volume as 0.522 m^3/g, and the pore size distribution analyzed by nitrogen adsorption-desorption measurement revealed that it had a two kind of pore structures with the diameter at 2.8 and 5.3 nm respectively. Both the mesopores sizes could be greatly in line with the requirements of the supercapacitors.[26] In contrast, the pore size distribution of pristine GO by freeze drying was mostly below 2 nm, and the specific surface area and pore volume were only as 32.9 m^2/g 0.046 m^3/g. As shown in Fig. S6a, WAXRD patterns of GO showed a common characteristic peak at about 10 °, which vanished after the pristine GO was solvent thermal treated. The DEG/graphene displayed broad and very weak peaks at 25 ° and 43 °, similar to other alcohol reduced RGO materials.[27] The diffraction maximum of DEG/graphene's SAXS patterns at about 1.6° denoted a layered structure with a spacing of about 5.2 nm in Fig. S4b, which was in conformity to the pore size distribution and the depth of individual DEG/graphene flake.

Electrochemical properties of DEG/graphene were measured both by cyclic voltammetry (CV) in the formation of two-electrode symmetrical coin cells with the 6M KOH alkaline solution as electrolyte. Fig. 3a shows the CV measurement results at different scanning rates varying from 2 and 200 mV/s. Whether at a relatively low scanning rate or high, all the CV curves exhibited symmetry and very approximate rectangular shape, suggesting the charge propagation of DEG/graphene was based on the electrochemical double layer charging mechanism which store energy using the adsorption of both anions and cations. That also means regrettably, although ether functionalities of DEG were introduced into the RGM, they hardly made a contribution to the capability by providing pseudo-capacitances. The CV curve rated at 200 mV/s expressed little distortion compared to that at 2 mV/s, which signified that the DEG/graphene was of good rate performance and power capability.[5a,28] The specific capacitances (*Cs*) against the scanning rate calculated by CV curves displayed in Fig 3c. As the scanning rate increased from 2 to 50 mV/s, *Cs* decreased from 230.3 F/g to 172.3 F/g. However, when scanning rate continued to increase, only a small decline was presented. The *Cs* kept as high as 152.9 F/g and 155.6 F/g at 100 and 200 mV/s, respectively. The relatively high retention of specific capacitance at high scanning rate (67.6% of the highest capacitance at 2 mV/s) offered this kind of materials more prospects for the practical application at high power densities. The CV curves and the calculated specific capacitance in the three-electrode system were showed in Fig. S7, which presented the similar situation as in the two-electrode system.

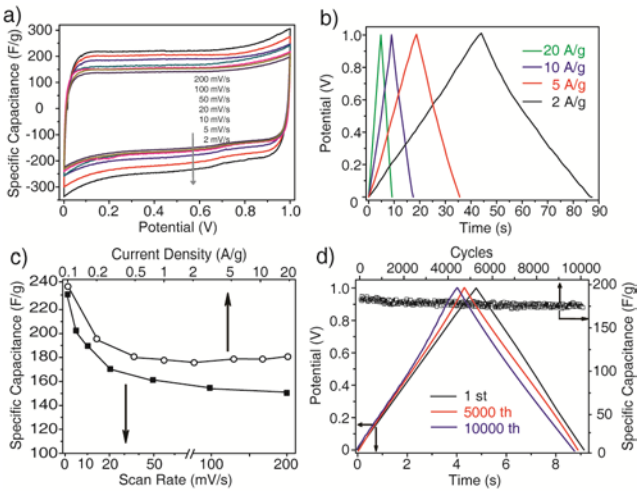

Fig. 3 Electrochemical properties of DEG/graphene supercapacitors electrodes in a 6M KOH solution. (a) CV curves at the scanning rate of 2-200 mV/s. (b) GC curves at the current densities of 2, 5, 10, and20 A/g. (c) the specific capacitances of DEG/graphene calculated by CV (bottom axis) and GC method (top axis), respectively. (d) GC curves of the 1st, 5000th, and 10000th (left and bottom axises), and the retention of *Cs* at 20 A/g (right and top axises).

Besides, series of two-electrode symmetrical coin cells in the same aqueous electrolyte has been fabricated to be tested by galvanostatic charge/discharge (GC), shown in Fig. 3b and S8. All the charging and discharging curve in the shape of straight line and symmetric triangle at different current densities reflected the good electric double-layer performance of DEG/graphene, suggesting no irreversible faradic processes are occurring during charging, which was in accordance with the results of cyclic voltammetry. The biggest calculated specific capacitance was 237.8 F/g when a low current density as 0.1 A/g was adopted. *Cs* dropped to 194.5 F/g and 179.7 F/g respectively with the increase of current to 0.2 and 0.5 A/g. A peculiar phenomenon was observed if the current density increased further, that the specific capacitance didn't decline any more. Even at a high current density as 20 A/g, the specific capacitance was measured as 182.9 F/g, a little higher than that at 0.5 A/g. The specific capacitances at other current densities could be acquired from Fig. 3c, that at 1, 2, 5, and 10 A/g were also at 180 F/g or so. After the appropriate reduction by a mild solvothermal treatment, DEG/graphene exhibited significantly increasing *Cs* than pristine GO (Fig. S9). Furthermore, the unexceptionable maintenance of capacitance against the magnification of charging current may be owed to excellent affinity of oxygen-containing groups with electrolyte

and the suitable pore structure allowing the ions in electrolyte to permeate rapidly.

The cycling durability of DEG/graphene in coin cells was investigated at these current densities over 1 A/g. As shown in Fig. 3d and S10, the cycling stability of DEG/graphene was documented to be excellent, with less than a 5% decrease at 1 A from the first cycle to the 2000th cycle. To be surprised, the cycling performance at higher current is better compared to that at 1 A/g. The cell device is able to retain about 98% of its capacitance at the end of every 2000th cycling test at 5, 10 and 20 A/g. Even after 10000 cycles, more than 90% of the capacitances were retained. The remarkableness of cycling stability of DEG/graphene in the wide range of high current densities was in coincidence with its satisfactory retention of specific capacitances at corresponding high current densities, both of which were supposed to be correlated with the collaboration of DEG functionalities, affording large specific surface area, adaptive mesoporosity and great electrolyte affinity. With such a unique integrated feature, the DEG/graphene RGM would be expected of an advantaged potential in application field.

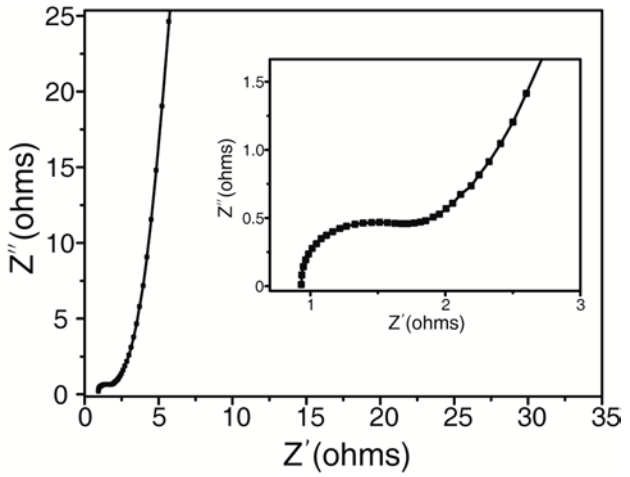

Fig. 4 Nyquist plots of two-electrode symmetrical coin cells of DEG/graphene supercapacitors electrodes. The inset is the close-up EIS image in the high frequency region.

Electrochemical impedance spectroscopy (EIS) was used to further evaluate the device performance of coin cell. As shown in the Nyquist plot (Fig. 4), DEG/graphene electrode exhibited a straight and nearly vertical line at low frequencies, confirming the excellent capacitive behavior of our supercapacitors.[29] The Warburg region at medium frequencies, representative of the diffusion/transport of electrolyte ions, was short, indicating that the diffusion/transport of electrolyte ions was improved by the introduction of suitable mesoporosity, as well as the accessibility of electrolytes to electrodes resulting from the existence of hydrophilic oxygen-containing functional group.[16,30] Only a depressed and small semicircle was observed at high frequencies in the amplifying Nyquist plot (as shown in inset of Fig. 4), and the equivalent series resistance (ESR) from the extrapolation of the vertical portion of the Nyquist plot to the real axis was estimated at 1.78 Ω, explaining that DEG/graphene materials had a comparatively good electrical conductivity after mild solvothermal reduction by diethylene glycol.[7,16] The highest energy density at the applied voltage of 1 V was 33.03 Wh/kg calculated by the formula $E = CsV^2/2$, and the maximum power density was 1.93 kW/kg by $P = V^2/4Rm$,[16] where V is the voltage applied, m is the total mass of the DEG/graphene electrodes (including the active materials and current collectors), Cs the measured device capacitance determined from galvanostatic charge, and R the equivalent series resistance.

Conclusions

In summary, diethylene glycol/graphene as supercapacitors electrodes material was fabricated by a simple and facile solvothermal treatment. The DEG molecules grafted into the surfaces of RGO mildly reduced by the alcohol, not only producing adaptive mesoporosity by preventing the aggregation of graphene as the "spacers", but also improving the wetting between graphene and electrolytes due to their hydrophilic nature. The DEG/graphene electrodes were provided with good electrochemical capacitances, as the greatest gravimetric capacitance reach 237.8 F/g at the current density of 0.1 A/g. Thanks to the smooth and swift passageways offered by the unique nanostructure, the electrodes played well at the higher charging current and cycling measurements. 182.9 F/g (75% of the biggest specific capacitance) was retained when the current density increased to as high as 20 A/g, and less than 5% was lost after 2000 cycles in the all measurements. These excellent features make it quite a promising materials a qualified electrode for supercapacitors, especially at high power densities.

Acknowledgements

We gratefully thank the Ministry of Science and Technology (2009CB930400, 2012CB932900), National Natural Science Foundation of China (NSFC21121063), and the Chinese Academy of Sciences (KJCX2-YW-N41) for financial support.

Notes and references

[a] *Laboratory of Molecular Nanostructures and Nanotechnology, Institute of Chemistry, Chinese Academy of Sciences & Beijing National Laboratory of Molecular Sciences, No.2 Zhongguancun North 1st Street, Beijing 100190, China. Fax&Tel: 86 10 6255 7908; E-mail: wsong@iccas.ac.cn*

[b] *University of Chinese Academy of Sciences, No.19A Yuquan Road, Beijing 100049,China.*

† Electronic Supplementary Information (ESI) available: (details of experimental section, XRD patterns, AFM image of GO, N_2 adsorption-desorption isotherm, more GC curves and cycling performances results). See DOI: 10.1039/b000000x/

1. Becker, H. I. F., V.; Low voltage electrolytic capacitor. US Patent 1957 2 800 616.
2. (a) K. S. Novoselov, A. K. Geim, S. V. Morozov, D. Jiang, Y. Zhang, S. V. Dubonos, I. V. Grigorieva and A. A. Firsov, *Science*, 2004, **306**, 666-669; (b) M. D. Stoller, S. Park, Y. Zhu, J. An and R. S. Ruoff, *Nano Lett*, 2008, **8**, 3498-3502. (c) S. Chen, W. Xing, J. Duan, X. Hu and S.-Z. Qiao, *J Mater Chem A*, 2013, **1**, 2941-2954.
3. (a) D.-W. Wang, F. Li, J. Zhao, W. Ren, Z.-G. Chen, J. Tan, Z.-S. Wu, I. Gentle, G. Q. Lu and H.-M. Cheng, *ACS Nano*, 2009, **3**, 1745-1752; (b) Q. Wu, Y. Xu, Z. Yao, A. Liu and G. Shi, *ACS Nano*, 2010, **4**, 1963-1970.
4. S. Biswas and L. T. Drzal, *Chem Mater*, 2010, **22**, 5667-5671.

5. (a) W. Lv, D.-M. Tang, Y.-B. He, C.-H. You, Z.-Q. Shi, X.-C. Chen, C.-M. Chen, P.-X. Hou, C. Liu and Q.-H. Yang, *ACS Nano*, 2009, **3**, 3730-3736; (b) Z.-S. Wu, W. Ren, L. Gao, J. Zhao, Z. Chen, B. Liu, D. Tang, B. Yu, C. Jiang and H.-M. Cheng, *ACS Nano*, 2009, **3**, 411-417.
6. J. J. Yoo, K. Balakrishnan, J. Huang, V. Meunier, B. G. Sumpter, A. Srivastava, M. Conway, A. L. Mohana Reddy, J. Yu, R. Vajtai and P. M. Ajayan, *Nano Lett*, 2011, **11**, 1423-1427.
7. X.-Z Wu, J Zhou, W. Xing, G.-G Wang, H.-Y Cui, S.-P Zhuo, Q.-Z Xue, Z.-F Yan, S.-Z Qiao, *J. Mater. Chem.*, 2012, **22**, 23186-23193.
8. Y. Zhu, S. Murali, M. D. Stoller, K. J. Ganesh, W. Cai, P. J. Ferreira, A. Pirkle, R. M. Wallace, K. A. Cychosz, M. Thommes, D. Su, E. A. Stach and R. S. Ruoff, *Science*, 2011, **332**, 1537-1541.
9. Y. Chen, X. Zhang, D. Zhang, P. Yu and Y. Ma, *Carbon*, 2011, **49**, 573-580.
10. Y. Huang, J. Liang and Y. Chen, *Small*, 2012, **8**, 1805-1834.
11. Y. Zhu, M. D. Stoller, W. Cai, A. Velamakanni, R. D. Piner, D. Chen and R. S. Ruoff, *ACS Nano*, 2010, **4**, 1227-1233.
12. Z. Lin, Y. Liu, Y. Yao, O. J. Hildreth, Z. Li, K. Moon and C.-p. Wong, *J Phys Chem C*, 2011, **115**, 7120-7125.
13. G. Wang, J. Yang, J. Park, X. Gou, B. Wang, H. Liu and J. Yao, *J Phys Chem C*, 2008, **112**, 8192-8195.
14. (a) X. Fan, W. Peng, Y. Li, X. Li, S. Wang, G. Zhang and F. Zhang, *Adv Mater*, 2008, **20**, 4490-4493; (b) Y. Xu, K. Sheng, C. Li and G. Shi, *ACS Nano*, 2010, **4**, 4324-4330.
15. C. Zhu, S. Guo, Y. Fang and S. Dong, *ACS Nano*, 2010, **4**, 2429-2437.
16. T. Y. Kim, H. W. Lee, M. Stoller, D. R. Dreyer, C. W. Bielawski, R. S. Ruoff and K. S. Suh, *ACS Nano*, 2010, **5**, 436-442.
17. J. Xu, K. Wang, S.-Z. Zu, B.-H. Han and Z. Wei, *ACS Nano*, 2010, **4**, 5019-5026.
18. M. J. McAllister, J.-L. Li, D. H. Adamson, H. C. Schniepp, A. A. Abdala, J. Liu, M. Herrera-Alonso, D. L. Milius, R. Car, R. K. Prud'homme and I. A. Aksay, *Chem Mater*, 2007, **19**, 4396-4404.
19. J. J. Tunney and C. Detellier, *Chem Mater*, 1996, **8**, 927-935.
20. N. A. Kumar, H.-J. Choi, Y. R. Shin, D. W. Chang, L. Dai and J.-B. Baek, *ACS Nano*, 2012, **6**, 1715-1723.
21. P. Harder, M. Grunze, R. Dahint, G. M. Whitesides and P. E. Laibinis, *J. Phys. Chem. B*, 1998, **102**, 426-436.
22. J. Chen, K. Sheng, P. Luo, C. Li and G. Shi, *Adv Mater*, 2012, **24**, 4569-4573.
23. (a) L. Li, S. Chen, J. Zheng, B. D. Ratner and S. Jiang, *J. Phys. Chem. B*, 2005, **109**, 2934-2941; (b) S.-Z. Zu and B.-H. Han, *J Phys Chem C*, 2009, **113**, 13651-13657.
24. (a) X. Li, T. Zhao, K. Wang, Y. Yang, J. Wei, F. Kang, D. Wu and H. Zhu, *Langmuir*, 2011, **27**, 12164-12171. (b) X. Li, T. Zhao, Q. Chen, P. Li, K. Wang, M. Zhong, J. Wei, D. Wu, B. Wei and H. Zhu, *Phys Chem Chem Phys*, 2013, **15**, 17752-17757.
25. Z. Lei, N. Christov and X. S. Zhao, *Energ Environ Sci*, 2011, **4**, 1866-1873.
26. (a) H. Shi, *Electrochim Acta*, 1996, **41**, 1633-1639; (b) D. Qu and H. Shi, *J Power Sources*, 1998, **74**, 99-107. (c) W. Xing, S.-Z. Qiao, R. G. Ding, F. Li, G. Q. Lu, Z.-F. Yan and H.-M. Cheng, *Carbon*, 2006, **44**, 216-224.
27. D. R. Dreyer, S. Murali, Y. Zhu, R. S. Ruoff and C. W. Bielawski, *J Mater Chem*, 2011, **21**, 3443-3447.
28. Z. Chen, J. Wen, C. Yan, L. Rice, H. Sohn, M. Shen, M. Cai, B. Dunn and Y. Lu, *Adv Energy Mater*, 2011, **1**, 551-556.
29. (a) K. Zhang, L. L. Zhang, X. S. Zhao and J. Wu, *Chem Mater*, 2010, **22**, 1392-1401; (b) Y. Li, Z. Li and P. K. Shen, *Adv Mater*, 2013, **25**, 2474-2480.
30. Z. Weng, Y. Su, D.-W. Wang, F. Li, J. Du and H.-M. Cheng, *Adv Energy Mater*, 2011, **1**, 917-922.

TOC Graphic and text:

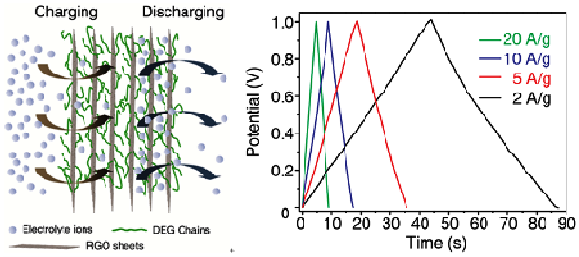

Graphene Based Composite Supercapacitor Electrodes with Diethylene glycol as Inter-layer Spacer